

fluoric acid and H_2O_2 (3–97%) and rinsed in distilled water and methanol a short while before implantation. After implantation, they were kept in dry atmosphere, but not in vacuum; this had no visible effect on the measured hyperfine field at room temperature, even after 6 months.

³²H. Frauenfelder and R. M. Steffen, in *α , β , γ Spectroscopy*, edited by K. Siegbahn (North-Holland, Amsterdam, 1964), Vol. II.

³³A. Abragam, *Principles of Nuclear Magnetism* (Oxford U. P., London, 1961).

³⁴H. Gabriel, *Phys. Letters* **32A**, 202 (1970).

³⁵As a further check on the model, we have also calculated R and A_1 including transverse relaxation. Though the transverse relaxation amplitude was varied from 0.1 to 10 times that of the longitudinal relaxation, no fit was obtained to the experimental result; in fact, the larger

C_1 and τ_1 , the worse the fit obtained.

³⁶Using $J_{sf} \sim 0.15$ eV (see Ref. 40), the corresponding magnetization of the Fe conduction electrons [Eq. (2.2)] is $\sim 0.15\mu_B$, in good agreement with the generally adopted value.

³⁷B. I. Deutch, in Ref. 6, p. 137; R. Alexander and L. C. Feldman (private communications).

³⁸L. C. Feldman *et al.*, *Phys. Rev. Letters* **27**, 1145 (1971); L. C. Feldman and D. E. Murnick, *Phys. Rev. B* **5**, 1 (1972); see also Ref. 6, Vol. 2, Session 3.

³⁹F. Abel, M. Bruneaux, C. Cohen, L. Thome, J. Chaumont, and H. Bernas (unpublished).

⁴⁰D. Davidov *et al.*, *Phys. Letters* **35A**, 339 (1971), and references therein.

⁴¹R. Jullien, A. Gomès, and B. Coqblin, *Phys. Rev. Letters* **29**, 482 (1972).

Finite-Size and Surface Effects in Heisenberg Films

Douglas S. Ritchie* and Michael E. Fisher

Baker Laboratory, Cornell University, Ithaca, New York 14850

(Received 9 June 1972)

High-temperature expansions for the zero-field susceptibility and specific heat to seventh order in $K=J/k_B T$ are reported for ferromagnetic Heisenberg-model simple-cubic-lattice "films" of $n=1, 2, \dots, 6$ layers. Extrapolation of the series yields reliable estimates of the susceptibility χ (and of the specific heats) down to temperatures at which $T\chi \approx 30(T\chi)_{T\infty}$. Firm conclusions about possible two-dimensional critical behavior cannot be reached, although the data are consistent with an exponent $\gamma_2=3.0 \pm 0.5$. The shifts of the apparent critical temperature $T_c(n)$ from the $d=3$ bulk value can be described by a power law $n^{-\lambda}$ with $\lambda \approx 1.1 \pm 0.2$. The surface susceptibility in the bulk limit diverges with an exponent $\gamma^x=2.18 \pm 0.02$ which appears to exceed the scaling prediction $\gamma^x=\gamma_3+\nu_3 \approx 2.08$; this could indicate the existence of a surface correlation length $\xi^x(T)$ with exponent $\nu^x > \nu_3$.

I. INTRODUCTION

It is well established that the dimensionality of a system plays a crucial role in determining its critical behavior. However, in order for the system to exhibit precisely the critical behavior characteristic of its dimensionality, it must be of infinite extent in all its dimensions. Restricting the size in one or more dimensions will affect the position and nature of the critical singularity (and may cause it to disappear). In the present investigation, which forms part of a general study of the effects of finite size on critical-point behavior,^{1–5} numerical results are obtained for ferromagnetic "films."

We consider a film consisting of n square-lattice layers stacked upon one another. The $n \times \infty \times \infty$ section of a simple cubic lattice so formed is infinite in two of its dimensions but of finite thickness na in the third dimension (where a is the nearest-neighbor lattice spacing). Two types of boundary conditions will be considered: *free surface*, where the surface spins each lack one neighboring site; and *periodic*, where the first and n th

layers are considered to be adjacent neighboring layers.

Allan² studied the corresponding spin- $\frac{1}{2}$ ferromagnetic Ising model and derived series expansions for the susceptibility $\chi_n(T)$ and specific heat $C_n(T)$. We have performed similar calculations for quantum-mechanical spins \vec{S}_i , on sites i , interacting through the isotropic Heisenberg Hamiltonian

$$\mathcal{H} = -\frac{J}{S^2} \sum_{(i,j)} \vec{S}_i \cdot \vec{S}_j - \frac{mH}{S} \sum_{i=1} S_i^z, \quad (1)$$

where the first sum runs only over distinct pairs of nearest-neighbor sites. We restrict attention to ferromagnetic ($J > 0$), nearest-neighbor coupling, but consider general values of the spin S . A preliminary account of this work has been published.⁵

We have extrapolated the series to study the "crossover" from three-dimensional behavior at high temperatures to two-dimensional behavior in the critical (or pseudocritical) region. The surface contribution to the susceptibility has also been calculated and its critical properties compared

with the general theories developed.³ Assuming there is a true critical point in two dimensions (at which the susceptibility diverges) the shifts in the critical temperature $T_c(n)$ for the n -layer film, from the bulk value ($n=\infty$) have been estimated. These shifts have also been examined in the light of the general theory, which we sketch very briefly in Sec. II.

II. GENERAL THEORY OF FINITE-SIZE EFFECTS

Suppose that the susceptibility $\chi_n(T)$ for the n -layer system diverges at a finite inverse critical temperature $K_c(n) = J/k_B T_c(n)$. The divergence will be characterized by a two-dimensional critical exponent γ_2 for all finite n , according to

$$\chi_n(K) \sim \{1 - [K/K_c(n)]\}^{-\gamma_2}, \quad (2)$$

as $K = J/k_B T - K_c(n)$ (n fixed).

However, for increasingly larger values of n the susceptibility will at first appear to diverge with the three-dimensional exponent γ_3 and will only "cross over" to this two-dimensional behavior closer and closer to the critical point $T_c(n)$. The effect of the finite thickness also appears in the deviation of the (inverse) critical temperature $K_c(n)$ from the bulk value $K_c(\infty)$. We may define a fractional shift

$$\epsilon(n) = [K_c(n) - K_c(\infty)]/K_c(\infty) \quad (3)$$

which, asymptotically for large n , is expected to vary as³

$$\epsilon(n) \approx b/n^\lambda \quad (n \rightarrow \infty). \quad (4)$$

With free-surface boundary conditions, there will be a surface contribution $\chi^s(T)$ to the total susceptibility per spin, $\chi_n(T)$. It is defined by the relation³

$$\chi_n(T) \approx \chi_\infty(T) + 2n^{-1}\chi^s(T) + \dots, \quad (5)$$

as $n \rightarrow \infty$, T fixed. The surface susceptibility will diverge at the bulk critical point, $K_c = K_c(\infty)$, according to

$$\chi^s(K) \sim [1 - (K/K_c)]^{-\gamma^s} \quad \text{as } K \rightarrow K_c, \quad (6)$$

The corresponding exponent γ^s will, in fact, be larger than the bulk exponent γ_3 .

Arguments can be advanced^{1,3} to relate the exponents λ and γ_3 to other known exponents. Thus a thorough-going scaling viewpoint suggests that the only relevant length with which to compare the film thickness $L = na$, is the bulk correlation length $\xi(T) \sim |K_c - K|^{-\nu_3}$. For free-surface films this leads to the predictions^{1,3}

$$\lambda = 1/\nu_3, \quad (7)$$

$$\gamma^s = \gamma_3 + \nu_3. \quad (8)$$

The first of these relations appears to hold quite

accurately for Ising-lattice films (with $\lambda \approx 1.56$).¹⁻³ On the other hand, one can also argue^{1,3} for the alternative (coupled) possibilities

$$\lambda = 1, \quad (9)$$

$$\gamma^s = \gamma_3 + 1. \quad (10)$$

These latter relations are, in fact, realized exactly in the spherical model and in ideal Bose gas films which can be analyzed rigorously for general dimensionality.⁴ However, in those models the values of λ and γ^s seem to be determined by some fairly special features of the models (namely, the existence of an over-all "constraint"). It is, thus, likely that (7) and (8) will apply more generally than (9) and (10). We shall compare our estimates for the Heisenberg films with these various expectations.

III. SERIES EXPANSIONS

The high-temperature expansions for the susceptibility and specific heat for general spin S have been calculated following the diagrammatic methods developed by Rushbrooke and Wood.⁶ The definitions (with regard to normalization with respect to spin) of a previous paper⁷ are followed here. In particular, the zero-field reduced susceptibility (for an n -layer lattice) is normalized by the paramagnetic susceptibility so that it approaches unity as $T \rightarrow \infty$, that is, we take

$$\chi_n(T) = \left(\frac{3S}{S+1} \right) \left(\frac{k_B T}{m^z} \right) \chi^{sz}(H=0, T), \quad (11)$$

where $\chi^{sz} = (\partial M^z / \partial H)_T$, and M^z is the z component of the magnetization. Seven terms in a power series in reduced inverse temperature, $K = J/k_B T$, have been obtained for the susceptibility

$$\chi_n(K) = 1 + \sum_{l=1}^{\infty} a_l^{(n)} K^l, \quad (12)$$

and for the specific heat,

$$\frac{C_n(K)}{k_B K^2} = \sum_{l=0}^{\infty} c_l^{(n)} K^l, \quad (13)$$

of an n -layer lattice with free surfaces, for $n=1, 2, \dots, 7$. The film with periodic boundary conditions is effectively "close packed" for small n and only six terms have been obtained in this case. The coefficients $a_l^{(n)}$ and $c_l^{(n)}$, which are polynomials of degree l in $X = S(S+1)$, are tabulated in Tables I and II. We will present only an outline of the calculation.

The specific heat is related to the partition function Z_N for N spins by

$$C(K) = N^{-1} k_B K^2 \left(\frac{\partial}{\partial K} \right)^2 (\ln Z_N). \quad (14)$$

A formal expression for the zero-field partition function is obtained by expanding the exponential

factor e^{-KP} , where

$$P = \sum_{(i,j)} \vec{S}_i \cdot \vec{S}_j, \tag{15}$$

about $K=0$ in the form

$$Z_N(K) = (2S+1)^N \left[1 + \sum_{l=2}^{\infty} \left(\frac{\langle P^l \rangle}{l! S^{2l}} \right) K^l \right], \tag{16}$$

where $\langle \circ \rangle = \text{Tr}\{\circ\}/(2S+1)^N$ denotes a reduced trace over the spin variables. Similarly, using the

TABLE I. Susceptibility coefficients. The polynomials $f_l^{(n)}(X)$ are listed; the susceptibility coefficients $a_l^{(n)}$, defined in Eq. (12), are related to these by $a_l^{(n)} = f_l^{(n)}(X)/2^l S^{2l}$ with $a_0^{(n)} = 1$ and $X = S(S+1)$.

Lattice	l	X	X^2	X^3	X^4	X^5	X^6	X^7
(i) Free surface								
$n=1$ (sq)	1	2.666667						
	2	-1.333333	5.333333					
	3	0.711111	-6.044444	9.955556				
	4	-0.444444	6.400000	-17.856790	16.908642			
	5	0.325079	-6.217143	27.600141	-43.208466	27.240447		
	6	-0.272593	6.254392	-39.126349	87.331593	-90.359020	42.212158	
	7	0.257354	-6.723725	52.358359	-159.709912	227.832174	-172.898878	63.067002
$n=2$	1	3.333333						
	2	-1.666667	8.888889					
	3	0.888889	-9.777778	22.814815				
	4	-0.555556	10.296296	-39.160494	55.308642			
	5	0.406349	-9.993651	58.564374	-132.338154	131.393768		
	6	-0.340741	10.058554	-81.802681	254.033533	-403.029935	301.729837	
	7	0.321693	-10.822434	108.803085	-446.878050	940.823712	-1147.073576	680.075597
$n=3$	1	3.555556						
	2	-1.777778	10.370370					
	3	0.948148	11.318519	29.471605				
	4	-0.592593	11.901235	-49.975309	80.065844			
	5	0.433439	-11.548783	74.140106	-188.262591	214.080815		
	6	-0.363457	11.625350	-103.155885	356.679287	-643.919012	557.017138	
	7	0.343139	-12.511041	136.976329	-621.477299	1477.480854	-2067.203071	1429.185966
$n=4$	1	3.666667						
	2	-1.833333	11.111111					
	3	0.977778	-12.088889	32.948148				
	4	-0.611111	12.703704	-55.555556	94.024691			
	5	0.446984	-12.326349	82.132910	-218.977072	265.314051		
	6	-0.374815	12.408748	-114.080635	412.097637	-788.056281	732.138428	
	7	0.353862	-13.355344	151.364868	-714.717805	1789.626202	-2673.825938	1998.246804
$n=5$	1	3.733333						
	2	-1.866667	11.555556					
	3	0.995556	-12.551111	35.034074				
	4	-0.622222	13.185185	-58.903704	102.479012			
	5	0.455111	-12.792889	86.928593	-237.511111	297.107490		
	6	-0.381630	12.878787	-120.635485	445.481651	-876.554334	845.133507	
	7	0.360296	-13.861926	159.997991	-770.828474	1980.037617	-3058.106416	2384.070686
$n=6$	1	3.777778						
	2	-1.888889	11.851852					
	3	1.007407	-12.859259	36.424691				
	4	-0.629630	13.506173	-61.135802	108.115226			
	5	0.460529	-13.103915	90.125714	-249.867137	318.347012		
	6	-0.386173	13.192146	-125.005385	467.737660	-935.618880	921.165892	
	7	0.364586	-14.199647	165.753406	-808.235586	2107.066840	-3315.756593	2647.471031
$n=7$	1	3.809524						
	2	-1.904762	12.063492					
	3	1.015873	-13.079365	37.417989				
	4	-0.634921	13.735450	-62.730159	112.141094			
	5	0.464399	-13.326077	92.409373	-258.692870	333.518099		
	6	-0.389418	13.415974	-128.126742	483.634810	-977.807842	975.499821	
	7	0.367649	-14.440877	169.864417	-834.954952	2197.801999	-3499.834239	2836.082356

TABLE I. (Continued)

Lattice	l	X	X^2	X^3	X^4	X^5	X^6	X^7
(ii) Periodic boundary conditions								
$n=2$	1	4.0						
	2	-2.0	12.444 444					
	3	1.066 667	-13.511 111	37.155 556				
	4	-0.666 667	14.192 593	-64.069 136	103.190 123			
	5	0.487 619	-13.770 159	94.516 261	-250.504 879	275.349 559		
	6	-0.408 889	13.862 716	-131.374 815	479.963 128	-873.871 056	704.867 380	
$n=3$	1	4.0						
	2	-2.0	13.333 333					
	3	1.066 667	-14.696 296	42.785 185				
	4	-0.666 667	15.377 778	-73.896 296	132.029 630			
	5	0.487 619	-14.931 640	110.016 508	-316.920 024	398.238 777		
	6	-0.408 889	15.063 704	-152.484 938	604.108 642	-1231.716 433	1174.362 250	
$n=4$	1	4.0						
	2	-2.0	13.333 333					
	3	1.066 667	-14.4	43.377 778				
	4	-0.666 667	15.111 111	-72.493 827	135.901 235			
	5	0.487 619	-14.659 048	106.387 866	-312.648 089	421.700 176		
	6	-0.408 889	14.758 942	-147.263 774	582.477 131	-1234.878 181	1281.262 191	
$n=5$	1	4.0						
	2	-2.0	13.333 333					
	3	1.066 667	-14.4	43.377 778				
	4	-0.666 667	15.111 111	-72.296 296	136.296 296			
	5	0.487 619	-14.659 048	106.111 323	-311.778 954	424.281 246		
	6	-0.408 889	14.758 942	-146.854 885	579.215 238	-1231.564 930	1299.607 102	

fluctuation relation, the zero-field susceptibility can be expressed as

$$\chi(K) = (2S+1)^N \left[1 + \sum_{l=1}^{\infty} \left(\frac{3\langle P^l Q^2 \rangle}{N! X S^{2l}} \right) K^l \right] / Z_N(K), \quad (17)$$

where $X = S(S+1)$ and

$$Q = \sum_{i=1}^N S_i^z. \quad (18)$$

The coefficients $\langle P^l \rangle$ can be represented as the sum over all l line graphs of the traces of the products of the spin operators $(\vec{S}_i \cdot \vec{S}_j)$ multiplied by the total lattice constant, i. e., the number of occurrences on the lattice of the graph formed by the bonds. The graphs for the susceptibility coefficients $\langle P^l Q^2 \rangle$ require two additional spin labels arising from the factor Q^2 . (These spin labels may be represented by two crosses on the graphs.)

The calculation then separates into two parts. Only spin traces with the two crosses on the same connected graph enter into the calculation of $\langle P^l Q^2 \rangle$: These are related to the coefficients $\langle P^l \rangle$ for unlabeled graphs (with lines only) by Theorem IV of Ref. 6. One can then utilize tables of sums of spin traces to calculate the required $\langle P^l \rangle$: We are indebted to Dr. P. J. Wood (of the University of Newcastle) for kindly sending us his unpublished data on the spin traces up to order $l=8$.

As usual, the dependence on lattice structure enters only through the lattice constants. For the connected graphs these were calculated with the aid of a computer program developed by Dr. J. L. Martin (of King's College, London). In this flexible program the lattice is specified by the set of nearest-neighbor vectors for each nonequivalent class of lattice points. Since one element of translational symmetry is lost in a finite layer lattice there are quite a few of these classes. The program then first generates a catalog of the self-avoiding walks (or chains) of one to four steps in length. This information is used to construct the various embeddings of the required graph in the lattice, by building up the graph in terms of the catalogued walks (rather than by adding single steps one at a time).

The separated diagrams were expressed in terms of connected graphs, by the standard symbolic techniques which determine the number of ways of overlapping the constituent pieces to form various connected graphs.⁸ In such extensive calculations every possible check must be made to avoid error. We were able to check our results against existing series^{8,9} for the regular ($n=1$ and $n=\infty$) lattices (sq, tri, sc, bcc, and fcc). Our data (to seventh order on the loose-packed lattices and sixth order on the close-packed lattices) check precisely in all cases. (A small discrepancy

was detected with the results given in Ref. 9 for the coefficient of X^7 in a_7 for the bcc lattice, which, however, the authors inform us is a misprint for 42334.1448. Our results confirm this and also agree with the $S=\infty$ calculations of Stanley,¹⁰ for this case.) We have also calculated the coefficients $a_i^{(n)}$ for $S=\infty$ using, where possible, Stanley's general relation in terms of the lattice constants of the appropriate (regular) lattice. This checked our general spin calculation and also served to lengthen the series for $S=\infty$. These additional series are

given in Table III.

Many of the lattice constants for the separated graphs could be checked individually against the published tabulations.⁸ Several of the lattice constants, including the finite film chains, were checked against previously calculated values (obtained by Allan for his work in extending Ref. 2). Finally, to sixth order we verified explicitly the cancellation of the contributions to $\ln Z_N$ and χ proportional to higher powers of N (N^2 , N^3 , ...), which arise from the separated graphs.

TABLE II. Specific-heat coefficients. The polynomials $g_i^{(n)}(X)$ are listed; the specific-heat coefficients $c_i^{(n)}$, defined in Eq. (13), are related to these by $c_i^{(n)} = zX^2 g_i^{(n)}(X) / 3(2^{i+1} S^{2i+4})$, where z is the mean coordination number which takes the values $z=4, 5, \frac{16}{3}, \frac{11}{2}, \frac{28}{5}, \frac{17}{3}, \dots$, 6 for $n=1, 2, 3, 4, 5, 6, \dots, \infty$.

	l	X^0	X^1	X^2	X^3	X^4	X^5	X^6
$n=1$ (sq)	0	1.0						
	1	-1.0	0.0					
	2	0.8	-4.8	1.866 667				
	3	-0.666 667	8.0	-2.074 074	0.0			
	4	0.609 524	-10.323 810	25.120 635	-12.867 725	-0.677 249		
	5	-0.613 333	12.8	-57.388 148	28.855 309	0.948 148	0.0	
	6	0.675 556	-16.327 111	101.869 037	-159.069 235	78.110 200	1.778 305	-2.415 320
$n=2$	0	1.0						
	1	-1.0	0.0					
	2	0.8	-6.133 333	3.466 667				
	3	-0.666 667	10.222 222	-3.851 852	0.0			
	4	0.609 524	-13.212 698	41.209 524	-31.949 206	15.204 233		
	5	-0.613 333	16.408 889	-93.56	67.709 630	-21.285 926	0.0	
	6	0.675 556	-20.963 556	166.097 541	-338.661 715	286.463 052	-179.121 901	41.143 028
$n=3$	0	1.0						
	1	-1.0	0.0					
	2	0.8	-6.633 333	3.866 667				
	3	-0.666 667	11.055 556	-4.296 296	0.0			
	4	0.609 524	-14.296 032	48.037 302	-39.460 318	20.656 085		
	5	-0.613 333	17.762 222	-109.392 963	83.254 815	-28.918 519	0.0	
	6	0.675 556	-22.702 222	194.481 778	-426.402 733	390.132 433	-272.494 442	88.413 410
$n=4$	0	1.0						
	1	-1.0	0.0					
	2	0.8	-6.860 606	4.048 485				
	3	-0.666 667	11.434 343	-4.498 317	0.0			
	4	0.609 524	-14.788 456	51.221 645	-42.874 459	23.134 199		
	5	-0.613 333	18.377 374	-116.778 316	90.320 808	-32.387 879	0.0	
	6	0.675 556	-23.492 525	207.713 401	-468.064 467	439.077 271	-316.724 260	110.793 825
$n=5$	0	1.0						
	1	-1.0	0.0					
	2	0.8	-6.990 476	4.152 381				
	3	-0.666 667	11.650 794	-4.613 757	0.0			
	4	0.609 524	-15.069 841	53.041 270	-44.825 397	24.550 265		
	5	-0.613 333	18.728 889	-120.998 519	94.358 519	-34.370 370	0.0	
	6	0.675 556	-23.944 127	215.274 328	-491.903 153	467.045 750	-341.998 442	123.582 633
$n=6$	0	1.0						
	1	-1.0	0.0					
	2	0.8	-7.074 510	4.219 608				
	3	-0.666 667	11.790 850	-4.688 453	0.0			
	4	0.609 524	-15.251 914	54.218 674	-46.087 768	25.466 542		
	5	-0.613 333	18.956 340	-123.729 237	96.971 155	-35.653 159	0.0	
	6	0.675 556	-24.236 340	220.166 693	-507.328 186	485.143 001	-358.352 324	131.857 744

TABLE III. Susceptibility coefficients $a_l^{(n)}$ for $S = \infty$.

	l	(sq) $n=1$	$n=2$	
Free-surface conditions	1	1.333 333 33	1.666 666 67	
	2	1.333 333 33	2.222 222 22	
	3	1.244 444 44	2.851 851 85	
	4	1.056 790 12	3.456 790 12	
	5	0.851 263 96	4.106 055 26	
	6	0.659 564 96	4.714 528 71	
	7	0.492 710 95	5.313 090 60	
	8	0.358 061 79	5.858 300 69	
	9	0.252 923 16	6.355 699 26	
	l	$n=3$	$n=4$	$n=5$
Periodic boundary conditions	1	2.0	2.0	2.0
	2	3.333 333 33	3.333 333 33	3.333 333 33
	3	5.348 148 15	5.422 222 22	5.422 222 22
	4	8.251 851 85	8.493 827 16	8.518 518 52
	5	12.444 961 79	13.178 130 51	13.258 788 95
	6	18.349 410 15	20.019 721 73	20.306 360 96
	7	26.532 900 65	30.182 323 08	30.875 799 60

IV. SURFACE SUSCEPTIBILITY

The surface susceptibility is defined in (5) asymptotically for large n ; however, the first seven terms in the high-temperature expansion for the (reduced) surface susceptibility

$$\chi^x(K) = \sum_{l=1}^{\infty} a_l^x K^l \quad (19)$$

can be determined exactly using the definition (5) formally with n equal only to 7. This follows from the observation that for any graph G_l of l lines, the difference between the bulk value of the lattice constant per site $(G_l)_\infty$, and that for n layers $(G_l)_n$, must satisfy

$$(G_l)_n - (G_l)_\infty = 2(G_l)^x/n \text{ for } n \geq l. \quad (20)$$

The surface lattice constant $(G_l)^x$ represents the number of ways a partially embedded graph can intersect the surface of a semi-infinite lattice, and hence fail to contribute to the over-all lattice constant. Thus when G_l is a connected graph the constant $(G_l)^x$ is negative.

This prescription was employed for $n=1, 2, \dots, 7$ and in all cases led to identical values of the surface coefficients a_l^x for $l \leq n$. The resulting coefficients for $l=1, 2, \dots, 7$ are listed in Table IV. Watson¹¹ has calculated the same series for spin $S = \frac{1}{2}$; unfortunately, his last two terms disagree with ours by small amounts. In view of our various crosschecks we believe our results are more trustworthy.

V. ANALYSIS OF SUSCEPTIBILITY SERIES

The first question to arise is the nature of the phase transition, if any, in two dimensions. Stanley and Kaplan^{12,13} have concluded, from an extrapolation of the high-temperature susceptibility series, for various plane ($n=1$) lattices that the susceptibility diverges at a nonzero temperature $T_c(1)$, even though there is known to be no long-range order below this "anomalous" critical point.¹⁴ From our analysis of the susceptibility series for the square lattice we do not feel able to reach such a definite conclusion. In particular, we find that the special expansion variable, $u = \coth K - (1/K)$, adopted by Stanley, does not seem to give appreciably better convergence. Thus, in Fig. 1 the residues of Padé approximants to $(d/du) \ln \chi_1(u)$ and $(d/dK) \ln \chi_1(K)$ are plotted against the value of the dominant pole in u and K , respectively. Data for the spin values of $S=1, \frac{3}{2}, \frac{5}{2}, \frac{9}{2}$, and ∞ are exhibited ($S = \frac{1}{2}$ being too ill-behaved for analysis). As can be seen, the residues, which should provide estimates of γ_2 , range from values of 1.5 to 4.5. Ratio plots are equally unsatisfactory: Figure 2 is a graph of the estimators $g_l = l(\mu_l/\mu_\infty - 1)$ for the exponent $(\gamma_2 - 1)$ for various assumed values of μ_∞ which give a reasonably horizontal plot for g_l vs $1/l$. (The expansion variable u is used here.) There is some indication of the spin dependence reported by Stanley and Kaplan¹² but, because of the large uncertainties, we do not believe it is very significant. Accordingly, we would estimate

$$\gamma_2 \approx 3.0 \pm 0.5 \text{ for all } S. \quad (21)$$

We must emphasize that this estimate is obtained

TABLE IV. Surface susceptibility. The polynomials $f_l^x(X)$ are listed; these are related to the surface-susceptibility coefficients a_l^x , defined in Eq. (19), by $a_l^x = f_l^x(X)/2^l S^{2l}$ with $a_0^x = 0$.

l	X	X^2	X^3	X^4	X^5	X^6	X^7
1	0.666 667						
2	-0.333 333	4.444 444					
3	0.177 778	-4.622 222	20.859 259				
4	-0.111 111	4.814 815	-35.481 481	84.543 210			
5	0.081 270	-4.665 397	47.956 825	-185.340 388	318.592 828		
6	-0.068 148	4.700 388	-65.548 501	333.840 141	-885.968 191	1141.012 518	
7	0.064 339	-5.065 820	86.331 231	-561.106 687	1905.438 343	-3865.630 567	3961.247 513

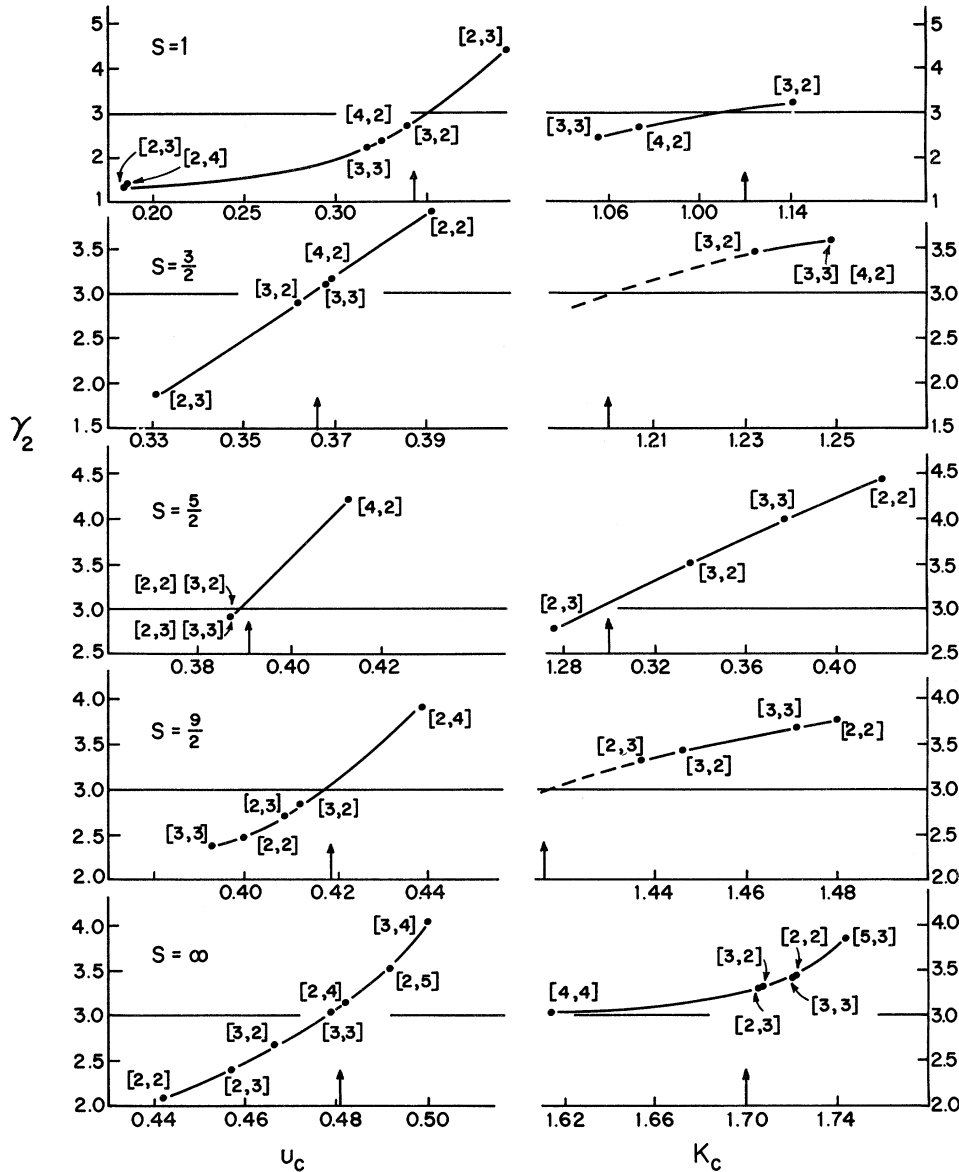


FIG. 1. Plot of the residues of the logarithmic derivative of the susceptibility series on the square lattice vs the corresponding pole. In the first column the expansion variable $u(T)$ was used while in the second the variable $K = J/k_B T$ was employed. The estimate ultimately adopted ($\gamma_2 = 3.0$) is indicated by a horizontal line. The corresponding estimated critical points are shown by a vertical arrow. The label $[D, N]$ indicates the particular Padé approximant employed.

from only the first seven terms of the series; the erratic behavior of the series casts some doubt on whether the susceptibility actually diverges at any nonzero temperature. Assuming, however, that $T_c(1)$ is positive, and that the divergence of $\chi_n(T)$ resembles a pure power law fairly closely, then (21) is a reasonable estimate of the exponent.

Once a value $\gamma_2 = 3.0$ is assumed for all finite thickness films³ ($n < \infty$) it is straightforward to obtain consistent estimates for the critical temperatures $T_c(n)$. The convergence (granted γ_2) is now comparatively good and the Padé and ratio techniques give consistent results in both variables u and K . A typical case is shown in Table V which lists the poles of Padé approximants to $[\chi_n(K)]^{1/\gamma_2}$ for $n = 4$ (free surfaces). The estimates from the

ratio plots are compared with the corresponding estimates from the Padé tables in Table VI. Our over-all conclusions for the dependence of $K_c(n) = J/k_B T_c(n)$ on n and S for both free-surface and periodic boundary conditions (assuming always that $\gamma_2 = 3.0$) are presented in Table VII.

Convenient numerical expressions for the susceptibility can now be obtained by dividing out the singular part of the susceptibility to obtain the amplitude function

$$A_n(K) = \chi_n(K) [1 - (K/K_c(n))]^{\gamma_2}, \tag{22}$$

Direct Padé approximants to $A_n(K)$ are found to be quite smoothly varying and hence provide explicit approximation formulae for $\chi_n(K)$. In Fig. 3 plots of the inverse susceptibility $[\chi_n(K)]^{-1}$ for spin

$S=1$, which were obtained using $\gamma_2=3.0$ and the appropriate $K_c(n)$, are shown for free-surface boundary conditions with $n=1, 2, \dots, 6$, and ∞ . Figure 4 gives an idea of the accuracy of such plots by comparing results obtained under the range of assumptions $\gamma_2=2.5, 3.0$, and 3.5 . Again the inverse susceptibility (now for spin $S=\infty$) is plotted using Padé approximants to the amplitude functions $A_n(K)$ appropriate to the various approximate critical points $K_c(n; \gamma_2)$. The curves coincide until the temperature has dropped to a value such that $[1 - (K/K_c(n))] \approx 0.2$, corresponding to a susceptibility of magnitude $\chi_n(K) \approx 70$. [Recall that by (11)

the reduced susceptibility is normalized such that $\chi_n(\infty)=1$.] Furthermore, the *direct* Padé approximants to the inverse susceptibility do not depend on any assumptions about the singularity but nevertheless coincide down to temperatures corresponding to $\chi_n(K) \approx 10$. We conclude, then, that one can calculate the susceptibility reliably over an appreciable temperature range without making any significant assumptions about the existence or nature of the singularity.

Figure 5 is a plot of $\log_{10} \chi_n(T)$ vs $\log_{10} \{[T/T_c(n)] - 1\}$ for spin $S=\infty$ in the case of free surfaces to study the appearance of the crossover from three-

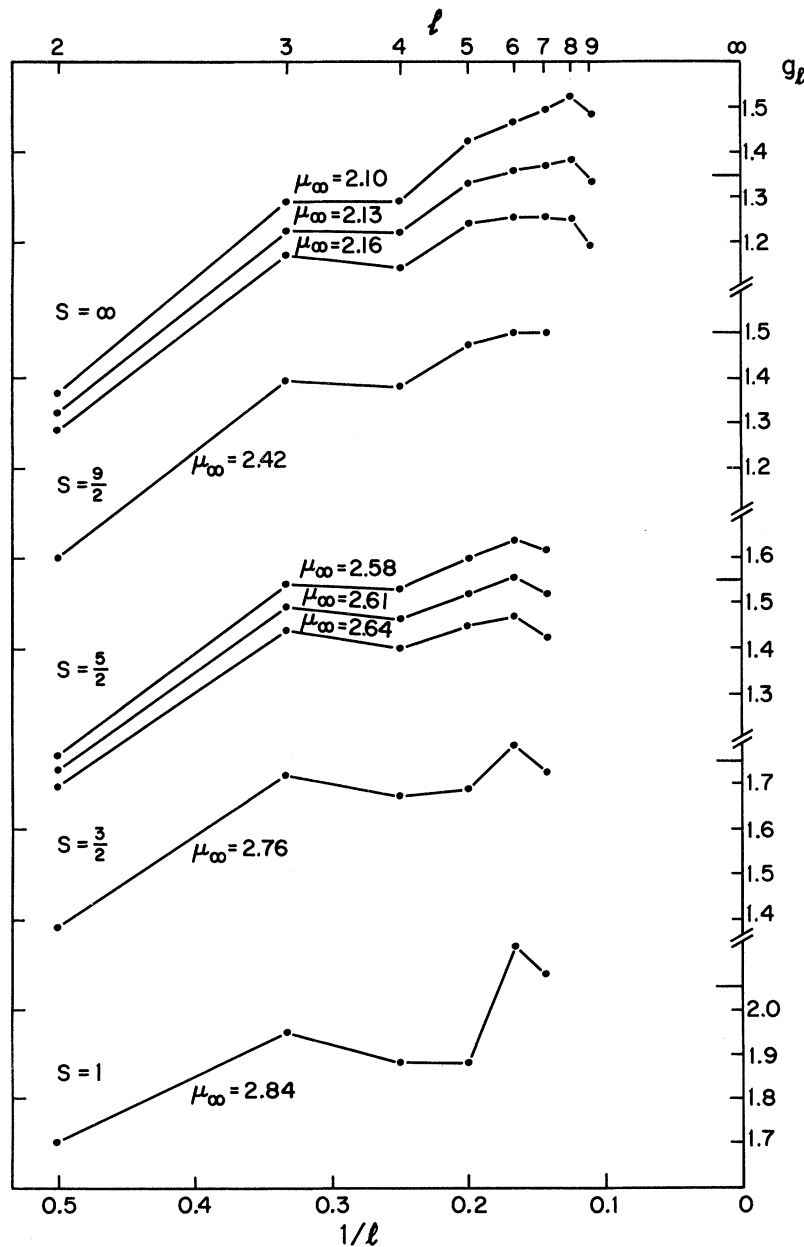


FIG. 2. Estimates $g_l = l(\mu_1/\mu_\infty - 1)$ for the susceptibility exponent $(\gamma_2 - 1)$ of the square lattice. The value for the critical temperature adopted is indicated on the plots. (The expansion variable u was used for this graph.)

TABLE V. Estimates of critical temperatures by Padé approximants. Roots of the approximants to $[\chi(u)]^{1/\gamma_2}$ and $[\chi(K)]^{1/\gamma_2}$ with $\gamma_2=3.0$ are listed for a lattice of $n=4$ layers with free-surface boundary conditions.

S	[D, N]	2	3	4	5
1	2	0.1683	0.1652	0.1613	0.1628
	3	0.1584	0.1607	0.1623	
	4	0.1609			
	5	0.1634		estimate	$u_c=0.162$
1/3	2	0.1903	0.1864	0.1822	0.1820
	3	0.1811	0.1814	0.1820	
	4	0.1814	0.1809		
	5	0.1822		estimate	$u_c=0.182$
1/5	2	0.2166	0.2122	0.2071	0.2063
	3	0.2068	0.2061	0.2059	
	4	0.2061	0.2059		
	5	0.2059		estimate	$u_c=0.206$
2/3	2	0.2418	0.2369	0.2311	0.2298
	3	0.2311	0.2298	0.2290	
	4	0.2299	0.2282		
	5	0.2291		estimate	$u_c=0.229$
8	2	0.2885	0.2821	0.2756	0.2739
	3	0.2758	0.2742	0.2722	
	4	0.2742			
	5	0.2728		estimate	$u_c=0.273$
1	2	0.5117	0.5046	0.4908	0.4966
	3	0.4816	0.4885	0.4942	
	4	0.4890			
	5	0.4986		estimate	$K_c=0.494$
1/3	2	0.5815	0.5719	0.5565	0.5570
	3	0.5536	0.5534	0.5570	
	4	0.5534	0.5536		
	5	0.5579		estimate	$K_c=0.557$
1/5	2	0.6652	0.6553	0.6362	0.6344
	3	0.6363	0.6319	0.6340	
	4	0.6320	0.6334		
	5	0.6340		estimate	$K_c=0.634$
2/3	2	0.7469	0.7369	0.7140	0.7110
	3	0.7157	0.7086	0.7099	
	4	0.7090	0.7097		
	5	0.7098		estimate	$K_c=0.710$
8	2	0.9029	0.8916	0.8627	0.8586
	3	0.8659	0.8559	0.8566	
	4	0.8565	0.8566		
	5	0.8566		estimate	$K_c=0.857$

TABLE VI. Critical temperatures for four-layer film. Results of the analysis of the four-layer (free-surface) series. Estimates of $k_B T_c/J$ are listed from (a) Padé to $[\chi(K)]^{1/3}$, (b) Padé to $[\chi(u)]^{1/3}$, (c) ratio estimate from $\chi(K)$, and (d) ratio estimate from $\chi(u)$.

S	(a)	(b)	(c)	(d)	Average
1	2.02	2.02	1.98	1.98	2.00
1/3	1.79 ₅	1.79 ₅	1.77 ₅	1.77	1.78
1/5	1.58	1.58	1.56 ₅	1.56 ₅	1.57
2/3	1.41	1.41	1.40	1.39	1.40
∞	1.17	1.16 ₅	1.16	1.14	1.16

dimensional behavior at high temperatures ($\gamma_3 \approx 1.38$) to two-dimensional behavior at lower temperatures ($\gamma_2 = 3.0$). Evidently on this plot, a clear changeover phenomena does not develop until larger values of n are reached than those for which we have complete data. Nevertheless it is clear that the characteristic two-dimensional slope sets in closer to $T_c(n)$ as n increases. (However, one must bear in mind that this plot will not be reliable numerically close to the estimated critical temperature.) Figure 6 shows how the critical amplitudes $A_c(n) = A_n(K_c(n))$ fall off with n . In fact, the scaling theory³ prediction that the reduced amplitude

$$A'_n = [K_c(n)/K_c(\infty)]^{\zeta} A_n(K_c(n)) \quad (23)$$

should vary as $n^{-\zeta}$, with $\zeta = (\gamma_2 - \gamma_3)/\nu_3 \approx 2.3$ (in this case), is found to hold fairly closely. Thus the solid lines in Fig. 6 correspond to values of $\zeta = 2.0$ and 2.3 for $S = \infty$ and 1 , respectively, with free-surface boundary conditions. The data for periodic conditions tend to suggest a larger exponent but they extend only to $n = 5$ and are subject to stronger "small- n effects" (see the following).

TABLE VII. Critical-temperature estimates. Estimates for the inverse critical temperature $K_c(n)$, based on the assumption $\gamma_2 = 3.0$ (with $\gamma_3 = 1.375$ for the $n = \infty$ lattice, Ref. 7). All entries in this table, except for the $n = \infty$ values, have an uncertainty of ± 0.01 .

(a) Free-surface Boundary Conditions							
S	n=1	2	3	4	5	6	∞
1	1.11 ₀	0.64 ₅	0.54 ₃	0.50 ₀	0.47 ₂	0.45 ₆	0.383
1/3	1.19 ₉	0.71 ₇	0.61 ₀	0.56 ₂	0.53 ₂	0.51 ₅	0.438 ₅
1/5	1.29 ₉	0.80 ₆	0.69 ₀	0.63 ₇	0.60 ₆	0.58 ₈	0.506 ₀
2/3	1.41 ₆	0.89 ₇	0.76 ₉	0.71 ₄	0.68 ₀	0.66 ₁	0.571
8	1.70 ₁	1.08 ₁	0.92 ₆	0.86 ₂	0.82 ₃	0.79 ₉	0.691 ₆
(b) Periodic boundary conditions							
S	n=2	3	4	5			
1	0.60 ₁	0.47 ₄	0.43 ₈	...			
1/3	0.66 ₃	0.53 ₂	0.49 ₈	...			
1/5	0.74 ₁	0.60 ₆	0.57 ₀	...			
2/3	0.82 ₀	0.68 ₁	0.64 ₁	...			
8	0.99 ₀	0.82 ₃	0.77 ₂	0.75 ₆			

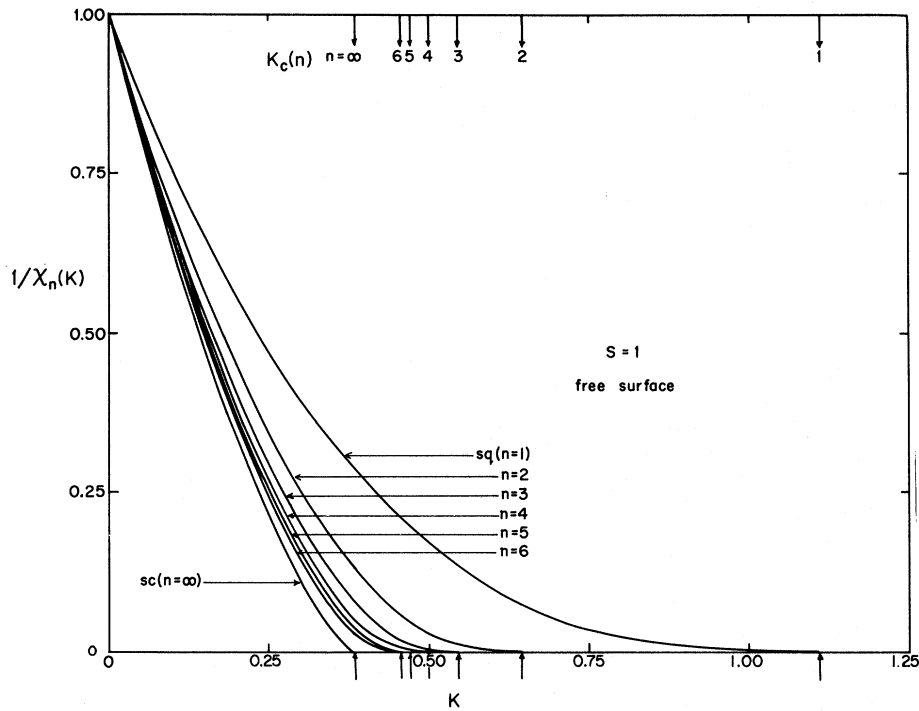


FIG. 3. The (reduced) inverse susceptibility $1/\chi_n(K)$ plotted vs inverse temperature $K=J/k_B T$ for spin $S=1$ and $n=1$ (sq), 2, 3, 4, 5, 6, and ∞ (sc) layers with free-surface boundary conditions. These plots assume a divergence with an exponent $\gamma_2=3.0$ (and $\gamma_3=1.375$ for the sc lattice).

VI. SPECIFIC-HEAT SERIES

Specific-heat series are normally quite difficult to analyze convincingly. Indeed we found it impossible to estimate the exponent α_2 , characterizing the (presumed) two-dimensional singularity, on the

basis of the standard straightforward methods. However, it is still useful to plot the specific heats since they can be measured experimentally. Direct Padé approximants to $C_n/k_B K^2$, which are plotted for spin- $\frac{5}{2}$ and free-surface conditions in Fig. 7, will be reliable only at the higher temperatures.

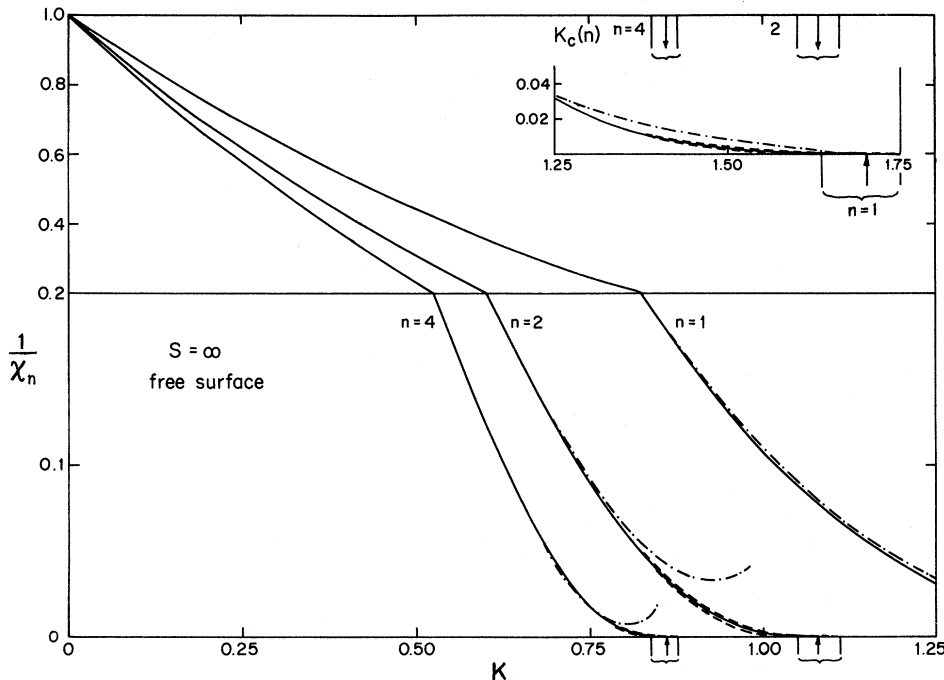


FIG. 4. Inverse susceptibility $1/\chi_n(K)$ vs K for $S=\infty$ and free-surface conditions. The accuracy of various approximants can be gauged: The solid line assumes a divergence with $\gamma_2=3.0$, the higher dashed line with $\gamma_2=3.5$, and the lower dashed line, with $\gamma_2=2.5$. The corresponding estimated critical points are indicated on the axes. In all these cases the best Padé approximants to the amplitude $A_n(K)=\chi_n(K)[1-(K/K_c)]^{\gamma_2}$ were used. Finally, the dot-dashed curve represents the direct Padé approximants to $1/\chi_n(K)$.

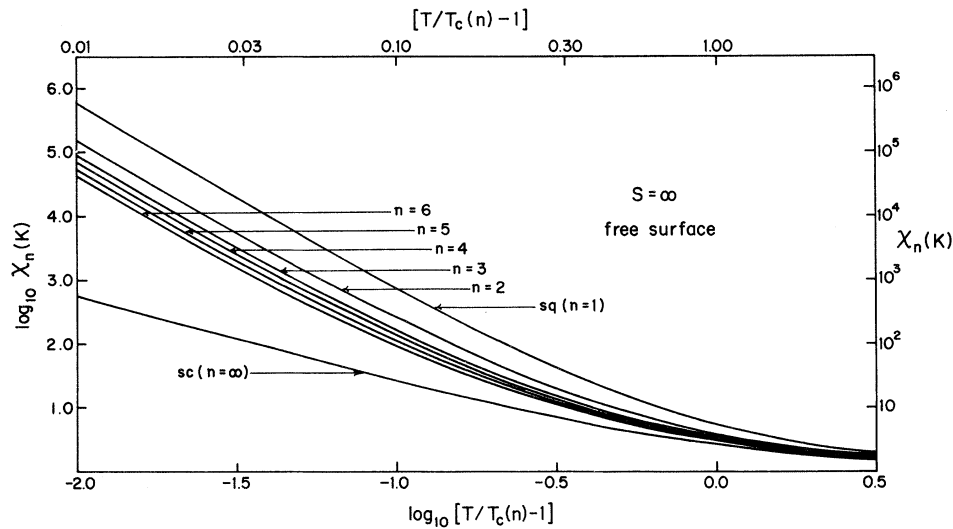


FIG. 5. Plot of $\log_{10} \chi_n(K)$ vs $\log_{10} \{ [T/T_c(n)] - 1 \}$ for $S = \infty$, to display the "cross-over" effect. [Padé approximants to $A_n(K)$ with $\gamma_2 = 3.0$ were used.]

These curves have been continued into the critical region in Fig. 7, merely to show qualitatively the variation with the number of layers. In order to obtain a more concrete idea of the accuracy of these plots, values of the partial sums, $\sum_{i=1}^N c_i^{(n)} K^{i-1}$, extrapolated versus $1/N$, are also shown. The two methods of extrapolation give approximately coincident results for the specific heats down to temperatures for which $[1 - (K/K_c(n))] \approx 0.3$ to 0.4 .

The specific-heat series for the lattice films have one especially interesting feature. In three dimensions, on the basis of series extrapolations and scaling arguments,⁷ the specific-heat exponent is thought to be negative, $\alpha_3 \approx -0.1$. Accordingly, the specific heat is finite at $T = T_c$, but has a sharp cusp there. Direct Padé approximants to the series cannot follow the sharp curvature of such a cusp at the critical temperature and, hence, tend to *overestimate* the inverse critical temperature K_c

and underestimate the critical value of the specific heat. However, the Padé approximants to the specific-heat series for finite n consistently exhibit a pole at a *smaller* value of K than the estimate, $K_c(n)$, of the inverse critical temperature obtained from the susceptibility series. In Table VIII these (real) poles are listed for $n = 2, 3, \dots, 6$, and ∞ and $S = \frac{5}{2}$ and ∞ . These Padé tables are surprisingly convergent for such a characteristically ill-behaved function. Such behavior, although based on very short series, is a little puzzling. It could possibly be an indication that the true specific-heat curve is rounded in the presumed critical region rather than displaying a cusp or divergence. In this case the Padé approximants, plotted in Fig. 7, would be significant overestimates of the true value in the critical region. With longer series one would then expect to find the pole "splitting" to form an imaginary pair, in the vicinity of which

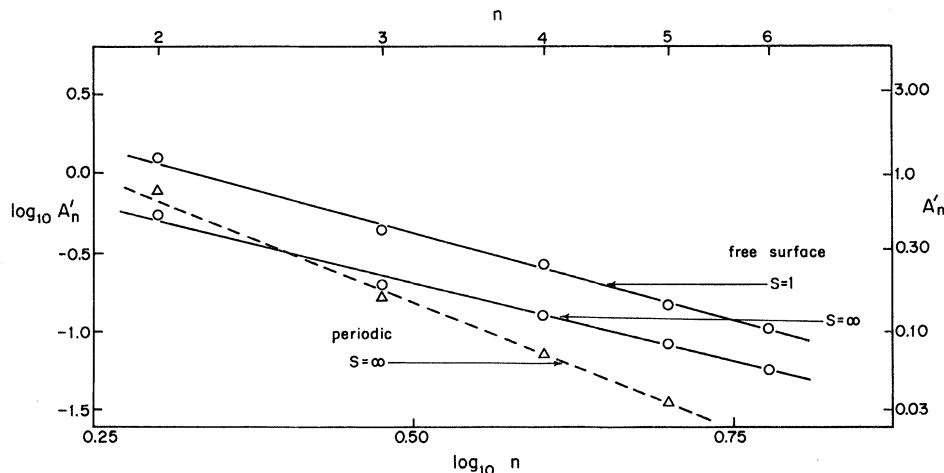


FIG. 6. Variation of the reduced critical amplitude A'_n , as defined in Eq. (22), for $S = 1$ and $S = \infty$.

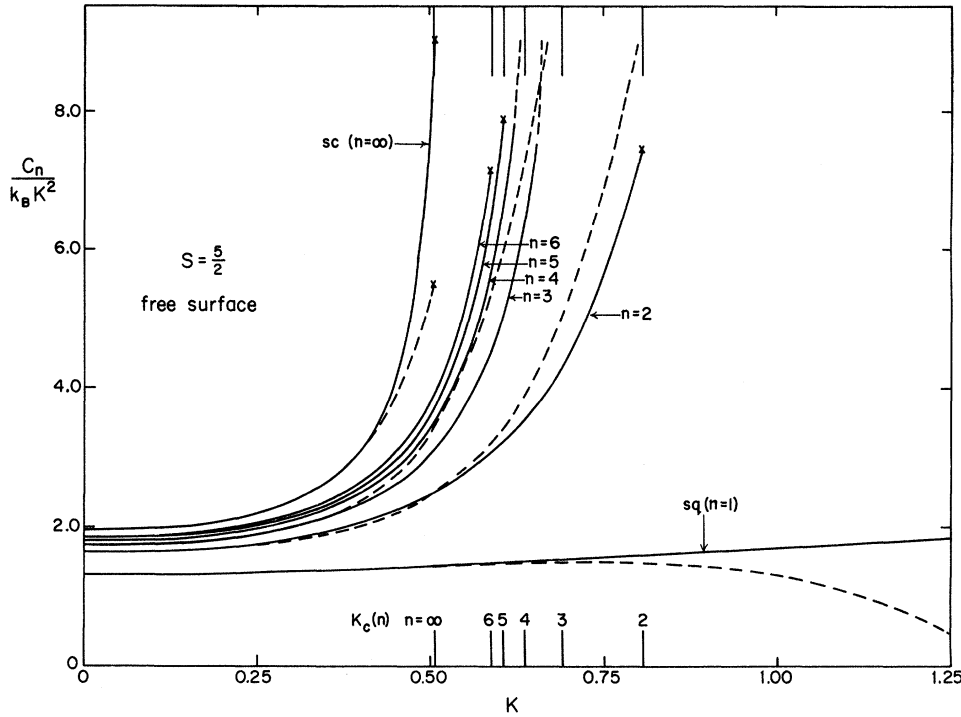


FIG. 7. Reduced specific heats $C_n(K)/k_B K^2$ vs inverse temperature K for $S = \frac{5}{2}$ and free-surface conditions. The solid lines represent direct Padé approximants; the dashed lines follow from extrapolation of the truncated series. The estimated critical points are indicated but the curves are merely qualitative near the corresponding critical point.

the specific heat would go through a rounded maximum above the estimated $T_c(n)$. Of course, this leaves quite open the question of the behavior of the specific heat at the critical point (if, indeed, one exists).

VII. SURFACE-SUSCEPTIBILITY ANALYSIS

We can be more definite about the properties of the surface susceptibility as the series, being essentially a bulk three-dimensional series, is comparatively well behaved. Using the bulk critical point $K_c = K_c(\infty)$, which is also quite accurately known,⁷ the standard ratio and Padé techniques were applied. The values of the Padé approximants to $(K - K_c)(d/dK) \ln \chi^x(K)$ evaluated at $K = K_c$ are presented in Table IX. The apparent convergence is good and we estimate

$$\gamma^x = 2.18 \pm 0.02 \quad (\text{all } S). \quad (24)$$

The error refers only to the apparent extrapolation uncertainties; the value would be shifted appreciably if the estimate for γ_3 [and hence for $K_c(\infty)$] were altered.

The estimated value of γ^x lies between the thorough-going scaling prediction (8), namely, $\gamma^x = \gamma_3 + \nu_3 \approx 2.08 \pm 0.03$, and the alternative prediction (10), namely, $\gamma^x = \gamma_3 + 1 \approx 2.38 \pm 0.02$. However, it is closer to the first, lower value. This situation is identical to that arising in the Ising model.³ At present we cannot reach any firm conclusions concerning these discrepancies. It may well be that

both powers ($\gamma_3 + \nu_3$) and ($\gamma_3 + 1$) are present, as actually predicted by the detailed scaling arguments³ when $\lambda = 1$. One might, alternatively, speculate that scaling theory breaks down for the surface properties in the sense that the $n = \infty$ bulk correlation length $\xi(T)$ may not be the only relevant

TABLE VIII. Specific-heat approximants. The smallest real poles of the direct Padé approximants to the specific heat $C_n(K)$ are listed. For $S = \infty$ the odd terms are not listed since the series then contains only even powers of K .

n	$[D, N]$	$S = \frac{5}{2}$			$K_c(n)$	$S = \infty$	
		2	3	4		2	4
2	2	0.673	0.690	1.051		0.955	1.216
	3	0.689	0.672		0.80 ₈		
	4	0.797				1.031	
3	2	0.605	0.621	0.758		0.865	0.967
	3	0.620	0.601		0.69 ₉		
	4	0.695				0.925	0.92 ₆
4	2	0.583	0.599	0.707		0.837	0.914
	3	0.598	0.580		0.63 ₇		
	4	0.663				0.888	0.86 ₂
5	2	0.573	0.588	0.686		0.823	0.891
	3	0.587	0.569		0.60 ₆		
	4	0.648				0.870	0.82 ₃
6	2	0.567	0.582	0.674		0.814	0.879
	3	0.581	0.563		0.58 ₈		
	4	0.640				0.860	0.79 ₉
∞ (sc)	2	0.543	0.557	0.636		0.781	0.835
	3	0.557	0.539		0.506 ₀		
	4	0.609				0.821	0.691 ₆

TABLE IX. Surface-susceptibility exponent. The values of Padé approximants to $[K - K_c(\infty)] (d/dK) \ln \chi^x(K)$ at $K = K_c(\infty)$.

S	[D, N]	1	2	3	4
1	1	2.12 ₃	2.14 ₁	2.22 ₆	2.20 ₀
	2	2.16 ₉	2.20 ₆	2.20 ₉	
	3	2.21 ₆	2.20 ₉		
	4	2.20 ₆			
2	1	2.09 ₂	2.15 ₅	2.19 ₆	2.18 ₃
	2	2.16 ₈	2.18 ₇	2.18 ₇	
	3	2.19 ₁	2.18 ₇		
	4	2.18 ₆			
3	1	2.07 ₃	2.15 ₆	2.18 ₇	2.18 ₀
	2	2.16 ₄	2.18 ₀	2.18 ₁	
	3	2.18 ₄	2.18 ₂		
	4	2.18 ₁			
4	1	2.06 ₈	2.15 ₇	2.18 ₇	2.18 ₄
	2	2.16 ₃	2.18 ₀	2.18 ₅	
	3	2.18 ₅	2.18 ₅		
	4	2.18 ₅			
8	1	2.05 ₈	2.15 ₂	2.18 ₁	2.17 ₈
	2	2.15 ₇	2.17 ₄	2.17 ₉	
	3	2.17 ₈	2.17 ₉		
	4	2.17 ₉			

diverging length. Thus, if there were some distinct surface correlation length $\xi^x(T)$, diverging with an exponent ν^x exceeding ν_3 , one could accept the relation $\gamma^x = \gamma_3 + \nu^x$ with the estimate $\nu^x \approx 0.80$ (whereas we have⁷ $\nu_3 \approx 0.70$). To develop such a viewpoint, one could argue that the surface susceptibility arises by reduction of the local susceptibility near the surface in a volume proportional to $A \xi^x(T)$ (where A is the free-surface area). This leads to

$$-\chi^x(T)/\chi_\infty(T) \approx \xi^x(T)/a. \quad (25)$$

The previous exponent (8) follows if we identify $\xi^x(T)$ with the bulk correlation length $\xi(T)$. To gain a feel for the magnitude of such a surface correlation length, the ratio $|\chi^x(T)/\chi_\infty(T)|$ and the (reduced) bulk correlation length $\xi_{(1)}(T)/a$ (defined from the second moment of the correlation function⁷) are plotted vs $[1 - (K/K_c)] = [1 - (T_c/T)]$ in Fig. 8. At high temperatures $\xi_{(1)}(T)$ behaves as $K^{1/2}$ whereas the ratio (χ^x/χ_∞) becomes proportional to K and hence is smaller than $(\xi_{(1)}/a)$. Close to the critical point, however, the curves should cross since $\nu^x > \nu_3$. In fact, the plots cross about 0.4% above T_c (as can be seen on the inset in Fig. 8). The numerical relationship between the two curves is probably still reliable in this temperature range so that if we take (25) as a definition of a surface

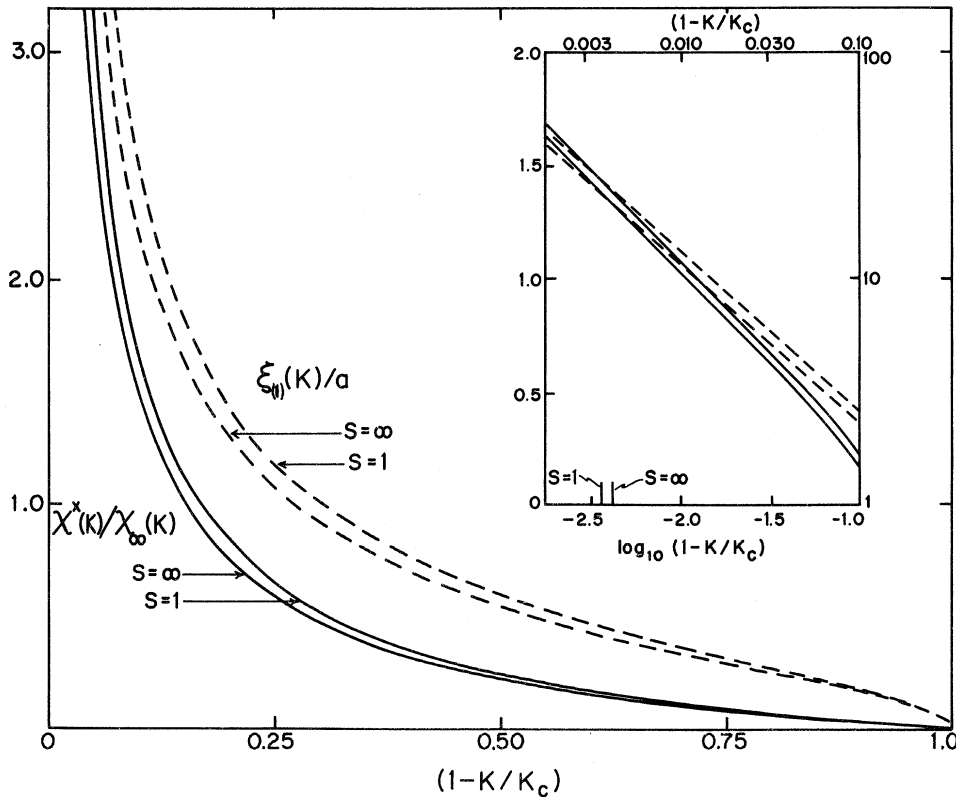


FIG. 8. Ratio of the surface susceptibility to the bulk susceptibility, $\chi^x(T)/\chi_\infty(T)$ (solid lines) and the (reduced) bulk correlation length $\xi_{(1)}(T)/a$ (dashed lines) derived from the second moment of the correlation function, for $S=1$ and $S=\infty$. The inset shows the behavior close to the critical point where the curves cross. [Padé approximants to the amplitude $A^x(K)$ with $\gamma^x = 2.18$ were used to calculate $\chi^x(T)$.]

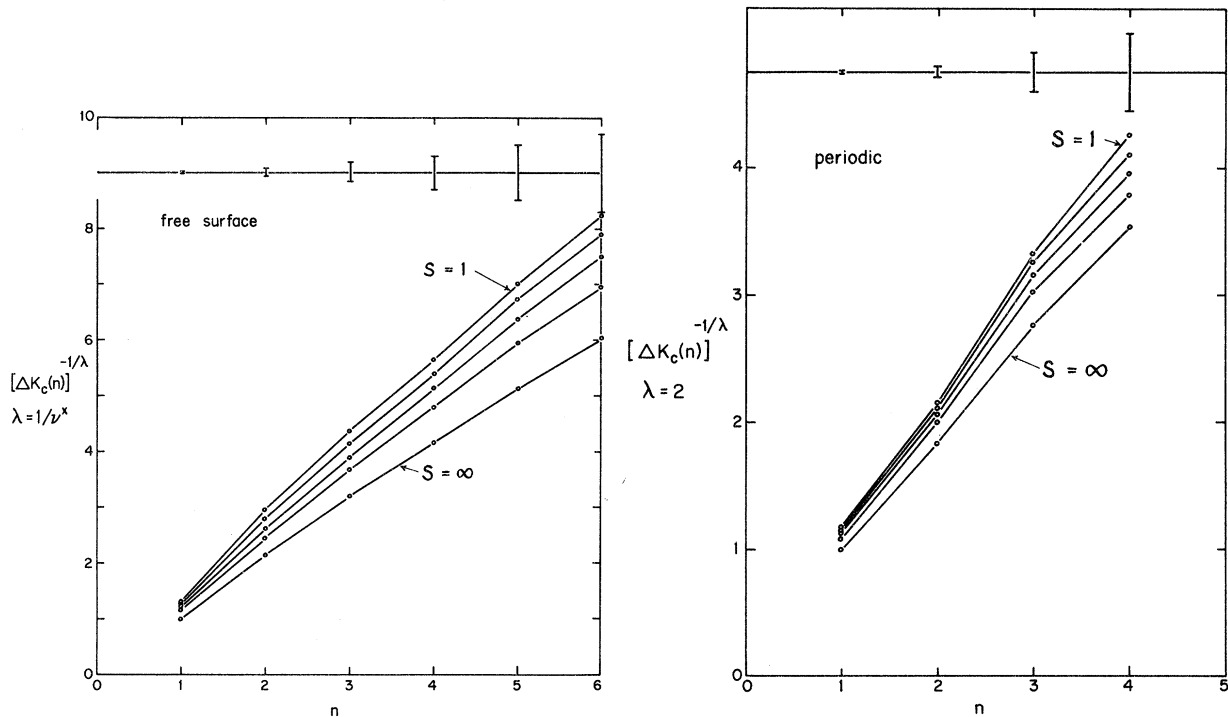


FIG. 9. Variation of critical temperature shift with n . The quantity $[\Delta K_c(n)]^{1/\lambda}$ is plotted, where $\Delta K_c(n) = K_c(n) - K_c(\infty)$, with (a), for free surfaces, $\lambda = 1/\nu^x$, and (b), for periodic conditions, $\lambda = 2$. The error bars at the top of the plots represent the range of uncertainty for each value of n .

correlation length $\xi^x(T)$ a sharper divergence does seem likely. However, there always remains the possibility that the correction terms to the leading divergence of $\chi^x(T)$ play an important role near T_c so that the asymptotic equality $\xi^x(T) \approx \xi(T)$ cannot, at this stage, be convincingly ruled out.

Finally, we might observe that if (25) is taken as a definition of $\xi^x(T)$ for spherical model and ideal Bose fluid films one always has $\nu^x = 1$ which exceeds ν_d for dimensions $d \geq 4$ (for which $\nu_d = \frac{1}{2}$).^{3,4}

VIII. CRITICAL-POINT SHIFTS

One of the main questions arising from the general theory of films is the value of the exponent λ , defined in (4), which determines the behavior of the critical-point shift for large n . Even in the event that a true critical point does not exist one may still expect to be able to define, more or less uniquely,^{3,4} a pseudocritical point which will vary in the corresponding way. Nevertheless, the estimates we will obtain depend fairly heavily on the assumption that a true critical point exists and that the susceptibility diverges there with an exponent $\gamma_2 \approx 3$.

To estimate λ , plots of $[K_c(n) - K_c(\infty)]^{-1/\lambda}$ vs n were made³ for various trial values of λ . The value which gives the most linear plot for the larger values of n provides the favored estimate. Note

that such a plot rightfully weights the higher n values more heavily. It might be expected that a Heisenberg model with short-range interactions would follow the scaling prediction $\lambda = 1/\nu_3$, as did the Ising model.^{2,3} However, this value of $\lambda (\approx 1.42)$ results in a noticeably curved plot. Figure 9(a) shows the plot with $\lambda \approx 1.24$ which corresponds to $\lambda \approx 1/\nu^x$ with $\nu^x = 0.80$, for the case of free-surface boundary conditions. A good straight-line fit can be obtained to the points with $2 \leq n \leq 6$. On the other hand, a reasonable straight-line fit to all the available points ($1 \leq n \leq 6$) can be found with $\lambda = 1.0$. This result is perhaps unexpected and should not be considered conclusive. Thus the critical points for the larger values of n could well be less accurate than suspected because of the difficulty of extrapolating the relatively short Heisenberg series. (Note also the uncertainties indicated at the top of the figure.) Indeed, we may recall that Allan² initially concluded that the value $\lambda = 1.0$ was consistent with his results for Ising films up to $n = 4$. However, later reanalysis,³ based on extended series for films of up to $n = 7$ layers, showed that $\lambda = 1/\nu_3$ gives a better fit than $\lambda = 1$. Accordingly, our tentative conclusion for the Heisenberg films may be stated as $\lambda = 1.1 \pm 0.2$.

With periodic boundary conditions the value $\lambda = 2$ gives a reasonable fit to the values $n = 1, 2, 3$, and

4. The corresponding plot of $[K_c(n) - K_c(\infty)]^{-1/\lambda}$ is shown in Fig. 9(b). The same value fits the Ising results also³ and similar large values are found for spherical model and ideal Bose films.⁴ No simple argument for these values has so far been constructed.

IX. CONCLUSIONS

In summary, we have not been able to conclude firmly whether or not the susceptibility of the plane square Heisenberg lattice diverges at a non-zero anomalous critical temperature. Indeed, there is indirect evidence that the specific heat may have a rounded peak in the region of suspected divergence of χ . Assuming that the susceptibility does diverge with an exponent $\gamma_2 \approx 2.5$ to 3.5 one can obtain reliable estimates of its magnitude down to temperatures at which the reduced susceptibility $T\chi^{**}/(T\chi^{**})_{T=\infty}$ attains a value around 70. Even with the assumption $\gamma_2 = 3.0$, however, the estimates of the critical points are insufficiently accurate or numerous to lead to precise estimates of the shift exponent λ : The data are consistent with the values $\lambda = 1$, $1/\nu^x \approx 1.24$, and, perhaps, although with less numerical plausibility, $\lambda = 1/\nu_3$.

The results for the surface susceptibility are more precise. As is the case for the $d=3$ Ising model, the exponent γ^x characterizing the divergence of the surface susceptibility appears to lie between the thorough-going scaling prediction γ_3

$+ \nu_3 \approx 2.08$, and the alternative prediction $\gamma_3 + 1 \approx 2.38$, at $\gamma^x \approx 2.18$. This has suggested the conjecture that there may be a different exponent $\nu^x \approx 0.80 > \nu_3 \approx 0.70$ characterizing a surface correlation length $\xi^x(T)$ which is distinct from the standard bulk correlation length. As noted, the prediction $\lambda = 1/\nu^x$ fits the results for the critical temperature shift $\epsilon(n)$ better than does the relation $\lambda = 1/\nu_3$.

In order to explore further some of the theoretical questions, we hope to extend these calculations to the Heisenberg-model transition from three to four dimensions, where there is no serious question regarding the existence of a sharp critical point $T_c(n)$. However, although the presently obtained data have proved hard to analyze in the immediate critical region, our numerical estimates for three-dimensional films still should be useful for comparison with experiments on uniform magnetic films above their transition temperatures.

ACKNOWLEDGMENTS

We are grateful for the support of the National Science Foundation and of the Advanced Research Projects Agency through the Materials Science Center at Cornell University. One of us (D. S. R.) is also grateful to Dr. J. W. Essam for his hospitality at Westfield College where this account was written. We are pleased to acknowledge again helpful correspondence with Dr. P. J. Wood.

*Present address: Department of Mathematics, Westfield College, London N.W. 3, England.

¹M. E. Fisher and A. E. Ferdinand, Phys. Rev. Letters **19**, 169 (1967); A. E. Ferdinand and M. E. Fisher, Phys. Rev. **185**, 832 (1969).

²G. A. T. Allan, Phys. Rev. B **1**, 352 (1970); for further extensions of this work, see Ref. 3.

³M. E. Fisher, *Theory of Critical Point Singularities V, Finite Size and Boundary Effects, Proceedings of the 1970 Enrico Fermi Summer School, Course No. 51, Varenna, Italy* (Academic, New York, 1972).

⁴G. A. T. Allan, M. N. Barber, M. E. Fisher, in Proceedings of the IUPAP Conference on Statistical Mechanics, Chicago, 1971 (unpublished); M. E. Fisher and M. N. Barber, Phys. Rev. Letters **28**, 1516 (1972); M. N. Barber and M. E. Fisher, Ann. Phys. (N. Y.) (to be published).

⁵D. S. Ritchie and M. E. Fisher, in *AIP Conference Proceedings No. 5, Magnetism and Magnetic Materials—1971* (AIP, New York, 1972), p. 1245; note that none of the figures in this paper are reproduced in the present

communication.

⁶G. S. Rushbrooke and P. J. Wood, Molec. Phys. **1**, 257 (1958).

⁷D. S. Ritchie and M. E. Fisher, Phys. Rev. B **5**, 2668 (1972) (note "approximately" in footnote 13d should read "appropriately").

⁸C. Domb, Advan. Phys. **9**, 149 (1960).

⁹R. L. Stephenson, K. Pirnie, P. J. Wood, and J. Eve, Phys. Letters **27A**, 2 (1968).

¹⁰H. E. Stanley, Phys. Rev. **158**, 546 (1967); **164**, 709 (1967).

¹¹P. G. Watson, Ph.D. thesis (University of London, London, 1968) (unpublished).

¹²H. E. Stanley and T. A. Kaplan, Phys. Rev. Letters **17**, 913 (1966); J. Appl. Phys. **38**, 975 (1967); **38**, 977 (1967).

¹³See also Refs. 10 above.

¹⁴N. D. Mermin and H. Wagner, Phys. Rev. Letters **17**, 1133 (1966); see also D. Jasnow and M. E. Fisher, *ibid.* **23**, 286 (1969); Phys. Rev. B **3**, 907 (1971).